

Third-Order Density Perturbation and One-Loop Power Spectrum in Dark-Energy-Dominated Universe

Ryuichi TAKAHASHI

Department of Physics and Astrophysics, Nagoya University, Nagoya 464-8602, Japan

We investigate the third-order density perturbation and the one-loop correction to the linear power spectrum in the dark-energy cosmological model. Our main interest is to understand the dark-energy effect on baryon acoustic oscillations in a quasi-nonlinear regime ($k \approx 0.1h/\text{Mpc}$). Analytical solutions and simple fitting formulae are presented for the dark-energy model with the general time-varying equation of state $w(a)$. It turns out that the power spectrum coincides with the approximate result based on the EdS (Einstein de-Sitter) model within 1% for $k < 0.4h/\text{Mpc}$ at $z = 0$ in the WMAP (Wilkinson Microwave Anisotropy Probe) 5yr best-fitting cosmological model, which suggests that the cosmological dependence is very small.

§1. Introduction

Revealing the nature of dark energy is fundamentally important not only for astrophysics but also for particle physics. Constraints on the dark energy from astronomical observations is very influential for them. Baryon acoustic oscillations (BAO) in the galaxy power spectrum provide a strong constraint on the dark energy using its acoustic scale as a standard ruler. Large galaxy surveys such as the Sloan Digital Sky Survey and two degree field already provide the constraint and future larger surveys are currently planned to detect the BAO more accurately.¹⁾⁻⁴⁾ Hence, an accurate theoretical model of the BAO is crucial, and many authors have been investigating the BAO using numerical simulation⁵⁾⁻¹¹⁾ and the perturbation theory (including the renormalized perturbation theory).¹³⁾⁻²¹⁾

Previously, several authors investigated the third-order density perturbation and derived the one-loop correction to the linear power spectrum in the EdS model.²³⁾⁻²⁸⁾ Similarly for the cosmological constant model, Bernardeau (1994) presented the third-order perturbation solution (see also Refs. 32)-36)). They found that the dependence of the cosmological model on the second- and third-order perturbations is very small, if the scale factor in the EdS model is replaced with the linear growth factor.^{*)} However, since the theoretical model of the BAO should archive the sub-percent accuracy to provide a strong constraint on the dark energy, it is useful to reinvestigate this topic to accurately check the above assumption. In this study, we calculate the third-order density perturbation, newly including the dark energy with the time-varying equation of state, and derive the one-loop power spectrum analytically for the first time. We compare our results with the approximate results based on the EdS model in detail, and discuss the effect of the dark energy on the power

*) Martel & Freudling (1991) and Scoccimarro et al. (1998) showed that this assumption is valid if $f \equiv d \ln D_1 / d \ln a = \Omega_M^{1/2}$. However, since $f \approx \Omega_M^{0.6}$, the approximation is not accurate.

spectrum near the baryon acoustic scale.

Throughout this paper, we use δ as the density fluctuation, $\theta (= \nabla \cdot \mathbf{v})$ as the divergence of the peculiar velocity field, and $\tau = a(t)dt$ as the conformal time. Ω_M , Ω_K and Ω_X are the density parameter for the matter, the curvature and the dark energy at present. $w(a)$ is the equation of state of the dark energy. The Hubble expansion rate is $H^2(a) = H_0^2 \left[\Omega_M a^{-3} + \Omega_K a^{-2} + \Omega_X \exp \left[3 \int_a^1 da' (1 + w(a')) / a' \right] \right]$.

§2. Basics

The equation of motion determines the growth of the density field $\delta(\mathbf{k}, \tau)$, and velocity field $\theta(\mathbf{k}, \tau) (\equiv i\mathbf{k} \cdot \mathbf{v}(\mathbf{k}, \tau))$ in the Fourier space is³¹⁾

$$\frac{\partial \delta(\mathbf{k}, \tau)}{\partial \tau} + \theta(\mathbf{k}, \tau) = - \int d^3 \mathbf{q} \alpha(\mathbf{q}, \mathbf{k} - \mathbf{q}) \theta(\mathbf{q}, \tau) \delta(\mathbf{k} - \mathbf{q}, \tau), \quad (2.1)$$

$$\begin{aligned} \frac{\partial \theta(\mathbf{k}, \tau)}{\partial \tau} + a(\tau) H(\tau) \theta(\mathbf{k}, \tau) + \frac{3}{2} a^2(\tau) \Omega_M(\tau) H^2(\tau) \delta(\mathbf{k}, \tau) \\ = - \int d^3 \mathbf{q} \beta(\mathbf{q}, \mathbf{k} - \mathbf{q}) \theta(\mathbf{q}, \tau) \theta(\mathbf{k} - \mathbf{q}, \tau), \end{aligned} \quad (2.2)$$

with

$$\alpha(\mathbf{p}, \mathbf{q}) = \frac{(\mathbf{p} + \mathbf{q}) \cdot \mathbf{p}}{p^2}, \quad \beta(\mathbf{p}, \mathbf{q}) = \frac{(\mathbf{p} + \mathbf{q})^2 \mathbf{p} \cdot \mathbf{q}}{2p^2 q^2}. \quad (2.3)$$

Equation (2.1) is the continuity equation, while equation (2.2) is the Euler equation with the Poisson equation. In the linear regime, one can neglect the mode-coupling terms on the right-hand sides of Eqs. (2.1) and (2.2). Then the linear solutions are

$$\delta_1(\mathbf{k}, a) = D_1(a) \delta_1(\mathbf{k}), \quad \theta_1(\mathbf{k}, a) = -a^2 H(a) \frac{dD_1(a)}{da} \delta_1(\mathbf{k}). \quad (2.4)$$

The linear growth factor $D_1(a)$ is determined by

$$\frac{d}{d^2 \ln a^2} \frac{D_1}{a} + \left(4 + \frac{d \ln H}{d \ln a} \right) \frac{d}{d \ln a} \frac{D_1}{a} + \left(3 + \frac{d \ln H}{d \ln a} - \frac{3}{2} \Omega_M(a) \right) \frac{D_1}{a} = 0, \quad (2.5)$$

with the initial condition $D_1(a)/a \rightarrow 1$ at $a \rightarrow 0$. In the special case of the flat model ($\Omega_K = 0$) with the constant w , the solution is given by the hypergeometric function.^{37), 38)}

The density field is formally expanded up to the third order as $\delta(\mathbf{k}, a) = \delta_1(\mathbf{k}, a) + \delta_2(\mathbf{k}, a) + \delta_3(\mathbf{k}, a)$. We will show the second- and third-order solutions in the following sections.

§3. Second-order solution

Inserting the linear-order solutions of δ_1 and θ_1 into the right-hand sides of equations (2.1) and (2.2), one can obtain the second-order solution as

$$\delta_2(\mathbf{k}, a) = D_{2A}(a) A(\mathbf{k}) + D_{2B}(a) B(\mathbf{k}), \quad (3.1)$$

with

$$A(\mathbf{k}) = \frac{5}{7} \int d^3 \mathbf{q} \alpha(\mathbf{q}, \mathbf{k} - \mathbf{q}) \delta_1(\mathbf{q}) \delta_1(\mathbf{k} - \mathbf{q}), \quad (3.2)$$

$$B(\mathbf{k}) = \frac{2}{7} \int d^3 \mathbf{q} \beta(\mathbf{q}, \mathbf{k} - \mathbf{q}) \delta_1(\mathbf{q}) \delta_1(\mathbf{k} - \mathbf{q}). \quad (3.3)$$

The second-order growth factors $D_{2A,B}$ are determined by ordinary differential equations with the boundary condition $D_{2A,B} \rightarrow a^2$ at $a \rightarrow 0$ (see Appendix A). One usually approximately use D_1^2 , instead of $D_{2A,B}$, in equation (3.1). In order to demonstrate the validity of this approximation, we show the relative differences between $D_{2A,B}$ and D_1^2 in Fig. 1 for the constant w in the flat model ($\Omega_K = 0$). The results are shown by the contour lines in the $\Omega_M - w$ plane for D_{2A} (top left panel) and D_{2B} (top right panel). As clearly seen in the figures, the relative errors are small, less than 4% for $0.1 < \Omega_M < 1$ and $-0.5 < w < -1.5$. The errors become larger for larger w . This tenancy suggests for larger w that the dark energy has been affecting the expansion rate since long time ago, and hence the large differences between $D_{2A,B}$ and D_1^2 arise at present.

Figure 2 is the same as Fig. 1, but for the time varying equation of state^{39),40)}

$$w(a) = w_0 + w_a a (1 - a). \quad (3.4)$$

The results are shown in the $w_0 - w_a$ plane with $\Omega_M = 0.28 (= 1 - \Omega_X)$. As shown in the figure, for large w_a , the relative differences become large. This is because the dark energy term in the hubble expansion $H^2(a)$, $\Omega_X a^{-3(1+w_0)} \exp[(3/2)w_a(1-a)^2]$, becomes large for large w_a in the past ($a < 1$). The relative errors are less than 10% for $-1.5 < w_0 < -0.5$ and $w_a < 3$.

§4. Third-order solution

Similarly, the third-order solution consists of six terms, as shown by

$$\begin{aligned} \delta_3(\mathbf{k}, a) = & D_{3AA}(a)C_{AA}(\mathbf{k}) + D'_{3AA}(a)C'_{AA}(\mathbf{k}) + D_{3AB}(a)C_{AB}(\mathbf{k}) \\ & + D'_{3AB}(a)C'_{AB}(\mathbf{k}) + D_{3BA}(a)C_{BA}(\mathbf{k}) + D_{3BB}(a)C_{BB}(\mathbf{k}), \end{aligned} \quad (4.1)$$

with

$$C_{AA}(\mathbf{k}) = \frac{7}{18} \int d^3 \mathbf{q} \alpha(\mathbf{q}, \mathbf{k} - \mathbf{q}) \delta_1(\mathbf{q}) A(\mathbf{k} - \mathbf{q}), \quad (4.2)$$

$$C'_{AA}(\mathbf{k}) = \frac{7}{30} \int d^3 \mathbf{q} \alpha(\mathbf{q}, \mathbf{k} - \mathbf{q}) \delta_1(\mathbf{k} - \mathbf{q}) A(\mathbf{q}), \quad (4.3)$$

$$C_{AB}(\mathbf{k}) = \frac{7}{18} \int d^3 \mathbf{q} \alpha(\mathbf{q}, \mathbf{k} - \mathbf{q}) \delta_1(\mathbf{q}) B(\mathbf{k} - \mathbf{q}), \quad (4.4)$$

$$C'_{AB}(\mathbf{k}) = \frac{7}{9} \int d^3 \mathbf{q} \alpha(\mathbf{q}, \mathbf{k} - \mathbf{q}) \delta_1(\mathbf{k} - \mathbf{q}) B(\mathbf{q}), \quad (4.5)$$

$$C_{BA}(\mathbf{k}) = \frac{2}{15} \int d^3 \mathbf{q} \beta(\mathbf{q}, \mathbf{k} - \mathbf{q}) \delta_1(\mathbf{q}) A(\mathbf{k} - \mathbf{q}), \quad (4.6)$$

$$C_{BB}(\mathbf{k}) = \frac{4}{9} \int d^3 \mathbf{q} \beta(\mathbf{q}, \mathbf{k} - \mathbf{q}) \delta_1(\mathbf{q}) B(\mathbf{k} - \mathbf{q}). \quad (4.7)$$

There are two additional conditions of

$$\begin{aligned} \frac{5}{18}D_{3AA} + \frac{2}{9}D'_{3AB} &= \frac{1}{2}D_1^3, \\ \frac{1}{6}D'_{3AA} + \frac{1}{9}D_{3AB} + \frac{2}{21}D_{3BA} + \frac{8}{63}D_{3BB} &= \frac{1}{2}D_1^3, \end{aligned} \quad (4.8)$$

and hence only four terms in Eq. (4.1) are independent of each other. The growth factors D_{3**} are determined by the ordinary differential equations with the boundary conditions of $D_{3**} \rightarrow a^3$ in $a \rightarrow 0$ (see Appendix A). The middle and bottom panels in Figs. 1 and 2 are the same as the top panels, but for the relative differences between D_{3**} and D_1^3 . The results are shown for D_{3AA} (middle left), D_{3AB} (middle right), D_{3BA} (bottom left), and D_{3BB} (bottom right). The relative differences are less than 7% for $0.1 < \Omega_M < 1$ and $-1.5 < w < -0.5$ and less than 20% for $-0.5 < w_0 < 0.5$ and $w_a < 3$.

Our results of the second- and third-order solutions are consistent with the previous results of Bernardeau (1994) for the cosmological constant model ($w = -1$). Although we presented the results for only the density perturbations, one can easily obtain the velocity field perturbations by inserting Eqs. (3.1) and (4.1) to Eqs. (2.1) and (2.2).

§5. One-loop power spectrum

The one-loop power spectrum is the linear power spectrum with the leading correction arising from the second- and third-order density perturbations,

$$\begin{aligned} P(k, a) &= \langle |\delta_1(k, a) + \delta_2(k, a) + \delta_3(k, a)|^2 \rangle \\ &= D_1^2(a)P_{11}(k) + P_{22}(k, a) + P_{13}(k, a), \end{aligned} \quad (5.1)$$

where $P_{11} = \langle |\delta_1|^2 \rangle$, $P_{22} = \langle |\delta_2|^2 \rangle$ and $P_{13} = \langle 2\text{Re}(\delta_1 \delta_3^*) \rangle$. The first term is the linear power spectrum, and the second and third terms are the one-loop corrections. The explicit formulae for P_{22} and P_{13} are given in Appendix B.

One usually approximately apply the one-loop power spectrum in the EdS model to an arbitrary cosmological model by replacing the scale factor by the linear growth factor,

$$P_{\text{EdS}}(k, a) = D_1^2(a)P_{11}(k) + D_1^4(a)[P_{22}(k) + P_{13}(k)]_{\text{EdS}}, \quad (5.2)$$

where the second and third terms are the corrections for the EdS model^{27),28)} (see also Appendix B). We compare the two power spectra in Eqs. (5.1) and (5.2) in order to quantitatively demonstrate the validity of the above approximation. We use CAMB (Code for Anisotropies in the Microwave Background)⁴¹⁾ to calculate the linear power spectrum with the cosmological parameters $h = 0.701$, $\Omega_B = 0.0462$, $\Omega_M = 0.279$, $n_s = 0.96$ and $\sigma_8 = 0.82$, consistent with the WMAP 5yr result.⁴²⁾

Figure 3 shows the relative differences in $P_{22}(k)$, $P_{13}(k)$, $P_{22}(k) + P_{13}(k)$ and $P(k)$ between Eqs. (5.1) and (5.2) at $z = 0$. The equation of states are $(w_0, w_a) = (-1.2, 0)$, $(-1, 0)$, $(-1, 2)$, and $(-0.8, 0)$. From the top panels, the error is $< 5\%$ for P_{13} while $\ll 1\%$ for P_{22} . On a small scale, these differences are small. In the

bottom left panel, the error diverges at $k \simeq 0.75h/\text{Mpc}$ because the denominator of $P_{22} + P_{13}$ vanishes there. The approximate formula of P_{EdS} predicts a slightly lower value than the correct result, because $[P_{22}]_{\text{EdS}} (> 0)$ is almost the same as P_{22} while $[P_{13}]_{\text{EdS}} (< 0)$ is more negative than P_{13} as shown in the top panels. However, as expected, the difference is very small at less than $\sim 1\%$ for $k < 0.4h/\text{Mpc}$. Figure 4 is the same as Fig. 3, but at various redshifts of $z = 0, 1, 3$. Hence, from this figure, the EdS model approximation in Eq. (5-2) is sufficiently more accurate for higher redshifts $z > 1$.

Finally, we calculate the shift in the position of the first acoustic peak at $k \simeq 0.07h/\text{Mpc}$. Dividing $P(k)$ by the no-wiggle model of Eisenstein & Hu (1999), we find that the position is shifted by only 0.8% (0.02%) for $z = 0$ ($z = 1$).

In this chapter, we calculated the one-loop power spectrum, however it is not accurate in the strong nonlinear regime ($k \gtrsim 0.1h/\text{Mpc}$). In fact, Jeong & Komatsu (2006) found that the one-loop power spectrum coincides with the nonlinear power spectrum from the numerical simulation within 1% if $\Delta^2(k) = k^3 P(k)/2\pi^2 < 0.4$ is satisfied. This condition is rewritten as $k < 0.12(0.26)h/\text{Mpc}$ at $z = 0$ ($z = 1$). Hence, in order to extend our analysis to a smaller scale, further analysis of the cosmological dependence of the higher-order perturbation theory is necessary.

§6. Conclusion

We investigate the third-order density perturbation and the one-loop power spectrum in the dark-energy cosmological model. We present analytical solutions and a fitting formula with the general time-varying equation of state for the first time. It turns out that the cosmological dependence is very weak, for example, less than 1% for $k < 0.4h/\text{Mpc}$ for the power spectrum. However, our results may be useful in some cases when one needs a very highly accurate theoretical model of the BAO or in the study of the nonlinear evolution on a smaller scale ($> 0.4h/\text{Mpc}$).

Acknowledgements

We would like to thank Takahiko Matsubara and the anonymous referees for helpful comments and suggestions. This work is supported in part by a Grant-in-Aid for Scientific Research on Priority Areas No. 467 “Probing the Dark Energy through an Extremely Wide and Deep Survey with Subaru Telescope”.

Appendix A

— Second- and Third-Order Growth Factors —

The second-order growth factors $D_{2A,B}$ are determined by the ordinary differential equations

$$\frac{d^2}{d \ln a^2} \frac{D_2}{a^2} + \left(6 + \frac{d \ln H}{d \ln a} \right) \frac{d}{d \ln a} \frac{D_2}{a^2} + \left[8 + 2 \frac{d \ln H}{d \ln a} - \frac{3}{2} \Omega_M(a) \right] \frac{D_2}{a^2}$$

$$= \frac{7}{5} \left[\left(\frac{dD_1}{da} \right)^2 + \frac{3}{2} \Omega_M(a) \left(\frac{D_1}{a} \right)^2 \right] \text{ for } D_{2A}, \quad (\text{A.1})$$

$$= \frac{7}{2} \left(\frac{dD_1}{da} \right)^2 \text{ for } D_{2B}, \quad (\text{A.2})$$

with the initial conditions at $a = 0$:

$$\frac{D_{2A,B}}{a^2} = 1, \quad \frac{d}{da} \frac{D_{2A,B}}{a^2} = 0. \quad (\text{A.3})$$

For the flat model with the constant equation of state, the solutions are well approximated as

$$D_{2A} \simeq D_1^2 \left[1 + |\ln \Omega_M| \left(\frac{5.54 \times 10^{-3}}{|w|} - \frac{3.40 \times 10^{-3}}{\sqrt{|w|}} \right) \right], \quad (\text{A.4})$$

$$D_{2B} \simeq D_1^2 \left[1 + |\ln \Omega_M| \left(-\frac{1.384 \times 10^{-2}}{|w|} + \frac{8.50 \times 10^{-3}}{\sqrt{|w|}} \right) \right], \quad (\text{A.5})$$

within a maximum error of 0.03% for both $0.1 \leq \Omega_M \leq 1$ and $-1.5 \leq w \leq -0.5$.

Similarly, the third-order growth factors are determined by

$$\begin{aligned} & \frac{d^2}{d \ln a^2} \frac{D_3}{a^3} + \left(8 + \frac{d \ln H}{d \ln a} \right) \frac{d}{d \ln a} \frac{D_3}{a^3} + \left[15 + 3 \frac{d \ln H}{d \ln a} - \frac{3}{2} \Omega_M(a) \right] \frac{D_3}{a^3} \\ &= \frac{18}{7} \left[2 \frac{dD_1}{da} + \frac{3}{2} \Omega_M(a) \frac{D_1}{a} \right] \frac{D_{2A,B}}{a^2} + \frac{18}{7} a \frac{dD_1}{da} \frac{d}{da} \frac{D_{2A,B}}{a^2} \text{ for } D_{3AA,3AB} \end{aligned} \quad (\text{A.6})$$

$$= 15 \frac{dD_1}{da} \left[a \frac{d}{da} \frac{D_{2A}}{a^2} + 2 \frac{D_{2A}}{a^2} - \frac{7}{5} \frac{D_1}{a} \frac{dD_1}{da} \right], \text{ for } D_{3BA} \quad (\text{A.7})$$

$$= \frac{9}{2} \frac{dD_1}{da} \left[a \frac{d}{da} \frac{D_{2B}}{a^2} + 2 \frac{D_{2B}}{a^2} \right], \text{ for } D_{3BB} \quad (\text{A.8})$$

with the initial conditions at $a = 0$:

$$\frac{D_3}{a^3} = 1, \quad \frac{d}{da} \frac{D_3}{a^3} = 0. \quad (\text{A.9})$$

For $\Omega_K = 0$ with the constant w , the solutions are well fitted by

$$D_{3AA} \simeq D_1^3 \left[1 + |\ln \Omega_M| \left(\frac{8.21 \times 10^{-3}}{|w|} - \frac{5.14 \times 10^{-3}}{\sqrt{|w|}} \right) \right], \quad (\text{A.10})$$

$$D_{3AB} \simeq D_1^3 \left[1 + |\ln \Omega_M|^{1.5+0.4 \ln |w|} |\Omega_M|^{0.7|w|} \left(-\frac{9.16 \times 10^{-3}}{|w|} + \frac{8.95 \times 10^{-3}}{\sqrt{|w|}} \right) \right], \quad (\text{A.11})$$

$$D_{3BA} \simeq D_1^3 \left[1 + |\ln \Omega_M|^{1.06-0.5 \ln |w|} \left(7.68 \times 10^{-3} |w| - 1.130 \times 10^{-2} \sqrt{|w|} \right) \right] \quad (\text{A}\cdot 12)$$

$$D_{3BB} \simeq D_1^3 \left[1 + |\ln \Omega_M| \left(-\frac{2.641 \times 10^{-2}}{|w|} + \frac{1.582 \times 10^{-2}}{\sqrt{|w|}} \right) \right], \quad (\text{A}\cdot 13)$$

within a maximum error of 0.05% for both $0.1 \leq \Omega_M \leq 1$ and $-1.5 \leq w \leq -0.5$. The other growth factors D'_{3AA} and D'_{3AB} can be obtained using Eq. (4.8).

Appendix B

— Explicit Expressions of P_{22} and P_{13} —

Here, we present the explicit expressions of the one-loop correction terms P_{22} and P_{13} . From the results in §3, we obtain

$$P_{22}(k, a) = \langle |\delta_2(\mathbf{k}, a)|^2 \rangle = D_{2A}^2(a) P_{2AA}(k) + 2D_{2A}(a) D_{2B}(a) P_{2AB}(k) + D_{2B}^2(a) P_{2BB}(k), \quad (\text{B}\cdot 1)$$

with

$$\begin{aligned} P_{2AA}(k) &= \frac{25}{392\pi^2} k^4 \int_0^\infty dk_1 \int_{-1}^1 d\mu P_{11}(k_1) P_{11} \left(\sqrt{k^2 + k_1^2 - 2kk_1\mu} \right) \left(\frac{k\mu + k_1 - 2k_1\mu^2}{k^2 + k_1^2 - 2kk_1\mu} \right)^2, \\ P_{2BB}(k) &= \frac{1}{98\pi^2} k^4 \int_0^\infty dk_1 \int_{-1}^1 d\mu P_{11}(k_1) P_{11} \left(\sqrt{k^2 + k_1^2 - 2kk_1\mu} \right) \left(\frac{k\mu - k_1}{k^2 + k_1^2 - 2kk_1\mu} \right)^2, \\ P_{2AB}(k) &= \frac{5}{196\pi^2} k^4 \int_0^\infty dk_1 \int_{-1}^1 d\mu P_{11}(k_1) P_{11} \left(\sqrt{k^2 + k_1^2 - 2kk_1\mu} \right) \frac{(k\mu - k_1)(k\mu + k_1 - 2k_1\mu^2)}{(k^2 + k_1^2 - 2kk_1\mu)^2}, \end{aligned}$$

where μ is the cosine between \mathbf{k} and \mathbf{k}_1 .

Similarly for P_{13} , from the results in §4, we obtain

$$\begin{aligned} P_{13}(k, a) &= \langle 2\text{Re}(\delta_1(\mathbf{k}, a)\delta_3^*(\mathbf{k}, a)) \rangle \\ &= D_{3AA}(a) P_{3AA}(k) + D'_{3AA}(a) P'_{3AA}(k) + D_{3AB}(a) P_{3AB}(k) \\ &\quad + D'_{3AB}(a) P'_{3AB}(k) + D_{3BA}(a) P_{3BA}(k) + P_{3BB}(a) P_{3BB}(k), \quad (\text{B}\cdot 2) \end{aligned}$$

with

$$\begin{aligned} P_{3AA}(k) &= -\frac{5}{54\pi^2} k^3 P_{11}(k) \int_0^\infty dr P_{11}(kr) (1 + r^2), \\ P'_{3AA}(k) &= \frac{1}{24\pi^2} k^3 P_{11}(k) \int_0^\infty dr P_{11}(kr) \left[1 + 4r^2 - r^4 + \frac{1}{2r} (r^2 - 1)^3 \ln \left| \frac{r+1}{r-1} \right| \right], \\ P_{3AB}(k) &= -\frac{1}{27\pi^2} k^3 P_{11}(k) \int_0^\infty dr P_{11}(kr) (1 + r^2), \\ P'_{3AB}(k) &= \frac{2}{27\pi^2} k^3 P_{11}(k) \int_0^\infty dr P_{11}(kr) r^2, \\ P_{3BA}(k) &= \frac{1}{168\pi^2} k^3 P_{11}(k) \int_0^\infty dr P_{11}(kr) \left[\frac{2}{r^2} (1 - 4r^2 - r^4) + \frac{(r^2 - 1)^3}{r^3} \ln \left| \frac{r+1}{r-1} \right| \right], \\ P_{3BB}(k) &= -\frac{4}{189\pi^2} k^3 P_{11}(k) \int_0^\infty dr P_{11}(kr). \end{aligned}$$

By setting $D_2 = a^2$ and $D_3 = a^3$ in Eqs. (B·1) and (B·2), the correction terms reduce to the result in the EdS model, $a^4[P_{22}(k) + P_{13}(k)]_{\text{EdS}}$.

References

- 1) D. J. Eisenstein et al., *Astrophys. J.* **633** (2005), 560.
- 2) S. Cole et al., *Mon. Not. R. Astron. Soc.* **362** (2005), 505.
- 3) W. J. Percival et al., *Mon. Not. R. Astron. Soc.* **381** (2007), 1053.
- 4) T. Okumura et al., *Astrophys. J.* **676** (2008), 889.
- 5) H. J. Seo and D. J. Eisenstein, *Astrophys. J.* **633** (2005), 575.
- 6) R. E. Angulo, C. M. Baugh, C. S. Frenk, and C. G. Lacey, *Mon. Not. R. Astron. Soc.* **383** (2008), 755.
- 7) E. Huff et al., *Astropart. Phys.* **26** (2007), 351.
- 8) R. E. Smith, R. Scoccimarro and R. K. Sheth, *Phys. Rev. D* **75** (2007), 063512.
- 9) R. E. Smith, R. Scoccimarro and R. K. Sheth, *Phys. Rev. D* **77** (2008), 043525.
- 10) R. Takahashi et al., *Mon. Not. R. Astron. Soc.* in press (2008), arXiv:0802.1808.
- 11) A. G. Sanchez, C. M. Baugh and R. Angulo, submitted to *Mon. Not. R. Astron. Soc.*, (2008), arXiv:0804.0233.
- 12) H.-J. Seo, E. R. Siegel, D. J. Eisenstein and M. White, submitted to *Astrophys. J.* (2008), arXiv:0805.0117.
- 13) D. Jeong and E. Komatsu, *Astrophys. J.* **651** (2006), 619.
- 14) M. Crocce and R. Scoccimarro, *Phys. Rev. D* **77** (2008), 023533.
- 15) M. Crocce and R. Scoccimarro, *Phys. Rev. D* **73** (2006), 063519.
- 16) T. Matsubara, *Phys. Rev. D* **77** (2008), 063530.
- 17) P. McDonald, *Phys. Rev. D* **75** (2007), 043514.
- 18) A. Taruya and T. Hiramatsu, *Astrophys. J.* **674** (2008), 617.
- 19) K. Izumi and J. Soda, *Phys. Rev. D* **76** (2007), 083517.
- 20) S. Matarrese and M. Pietroni, *J. Cosmol. Astropart. Phys.* **06** (2007), 026.
- 21) T. Nishimichi et al., *Publ. Astron. Soc. Jpn.* **59** (2007), 1049.
- 22) D. Jeong and E. Komatsu, arXiv:0805.2632.
- 23) R. Juszkiewicz, *Mon. Not. R. Astron. Soc.* **197** (1981), 931.
- 24) E. T. Vishniac, *Mon. Not. R. Astron. Soc.* **203** (1983), 345.
- 25) M. H. Goroff, B. Grinstein, S. J. Rey and M. B. Wise, *Astrophys. J.* **311** (1986), 1.
- 26) Y. Suto and M. Sasaki, *Phys. Rev. Lett.* **21** (1991), 264.
- 27) N. Makino, M. Sasaki and Y. Suto, *Phys. Rev. D* **46** (1992), 585.
- 28) B. Jain and E. Bertschinger, *Astrophys. J.* **431** (1994), 495.
- 29) H. Martel and W. Freudling, *Astrophys. J.* **371** (1991), 1.
- 30) R. Scoccimarro et al., *Astrophys. J.* **496** (1998), 586.
- 31) F. Bernardeau, S. Colombi, E. Gaztanaga and R. Scoccimarro, *Phys. Rep.* **367** (2002), 1.
- 32) F. R. Bouchet, R. Juszkiewicz, S. Colombi and R. Pellat, *Astrophys. J.* **394** (1992), L5.
- 33) F. Bernardeau, *Astrophys. J.* **433** (1994), 1.
- 34) F. R. Bouchet, S. Colombi, E. Hivon and R. Juszkiewicz, *Astron. Astrophys.* **296** (1995), 575.
- 35) P. Catelan, F. Lucchin, S. Matarrese and L. Moscardini, *Mon. Not. R. Astron. Soc.* **276** (1995), 39.
- 36) T. Matsubara, *Prog. Theor. Phys.* **94** (1995), 1151.
- 37) V. Silveira & I. Waga, *Phys. Rev. D* **50** (1994), 4890.
- 38) T. Padmanabhan, *Phys. Rep.* **380** (2003), 235.
- 39) M. Chevallier and D. Polarski, *Int. J. Mod. Phys. D* **10** (2001), 213.
- 40) H. K. Jassal, J. S. Bagla and T. Padmanabhan, *Mon. Not. R. Astron. Soc.* **356** (2005), L11.
- 41) A. Lewis, A. Challinor and A. Lasenby, *Astrophys. J.* **538** (2000), 473.
- 42) E. Komatsu et al., submitted to *Astrophys. J. Suppl.* arXiv:0803.0547.
- 43) D.J. Eisenstein and W. Hu, *Astrophys. J.* **511** (1999), 5.

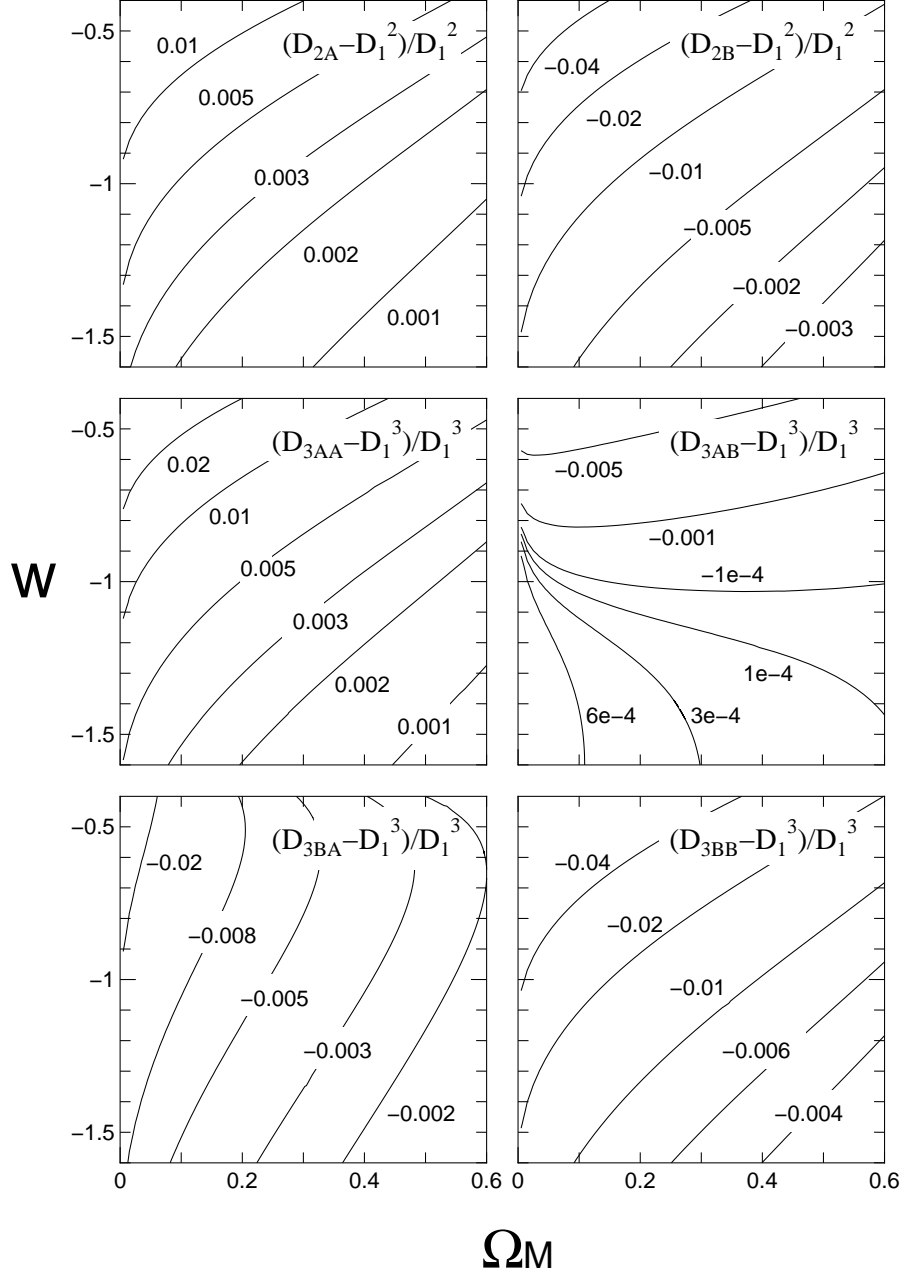


Fig. 1. Top panels: the contour lines show the relative differences between $D_{2A,B}$ and D_1^2 at present ($a = 1$) in the $\Omega_M - w$ plane. The flat cosmological model and the constant equation of state are assumed. The top left (right) panel is the result for D_{2A} (D_{2B}). Middle and bottom panels: same as top panels, but for the relative differences between D_3 and D_1^3 .

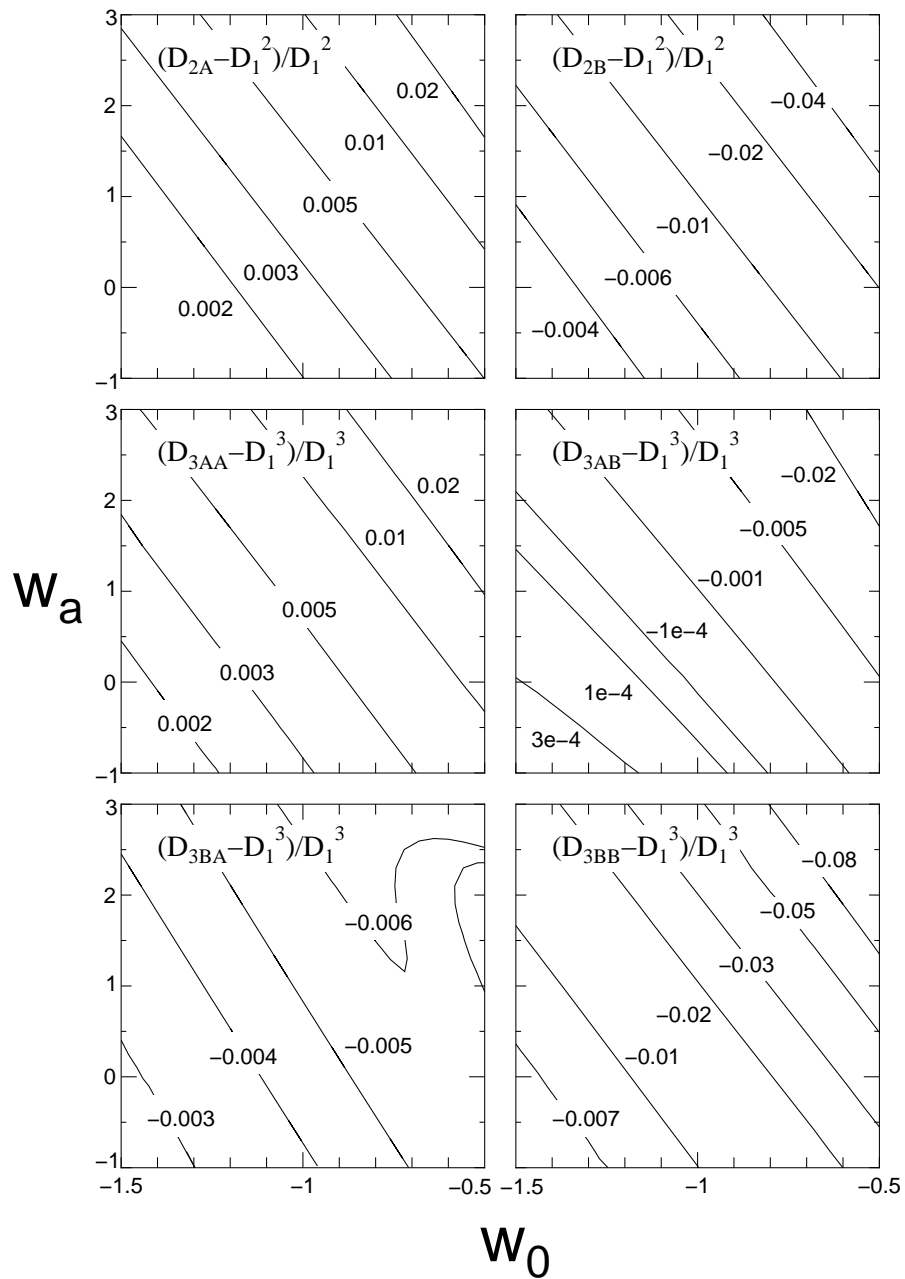


Fig. 2. Same as Fig. 1, but for the time-varying equation of state, $w(a) = w_0 + w_a a(1 - a)$. The results are shown in the $w_0 - w_a$ plane in the flat cosmological model with $\Omega_M = 0.28$.

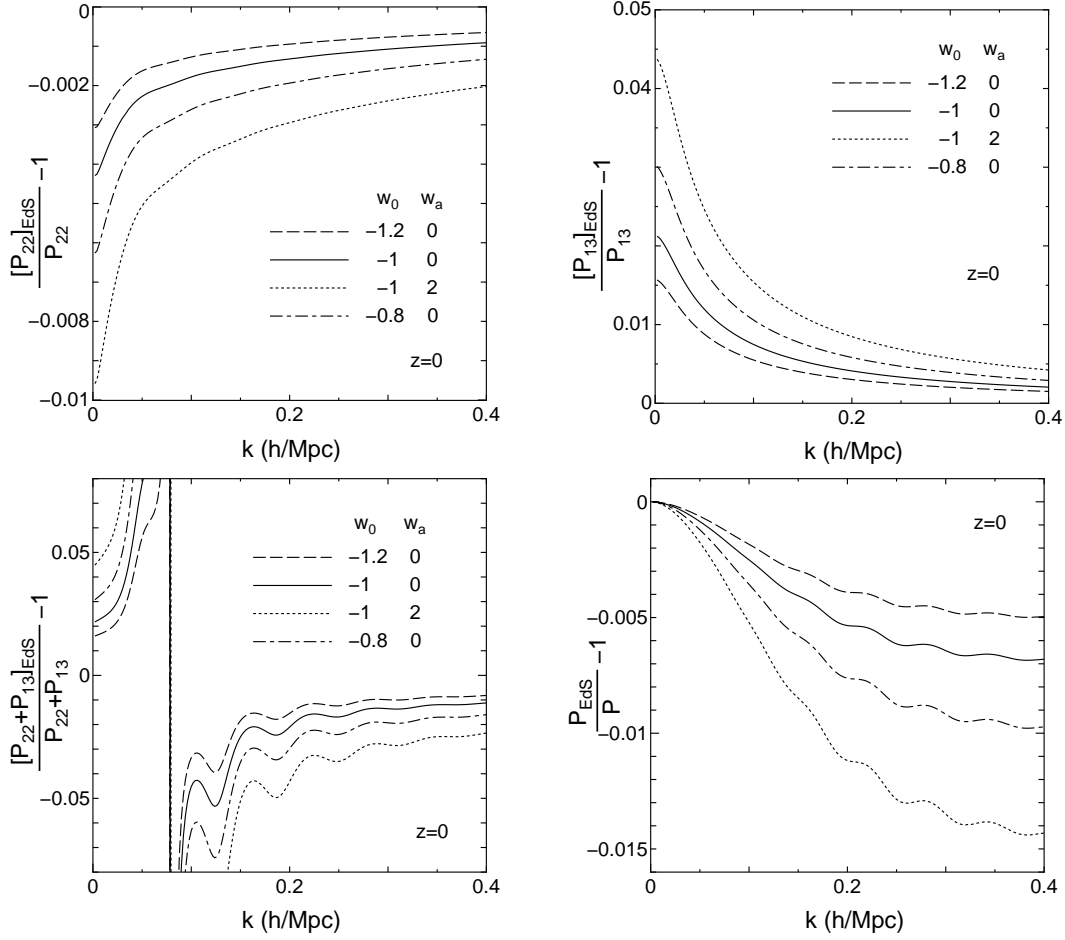


Fig. 3. Relative differences of $P_{22}(k)$ (top left), $P_{13}(k)$ (top right), $P_{22}(k) + P_{13}(k)$ (bottom left) and $P(k)$ (bottom right) between the correct results and the approximate results denoted by $[\dots]_{\text{EdS}}$. The cosmological model is consistent with the WMAP 5yr result.

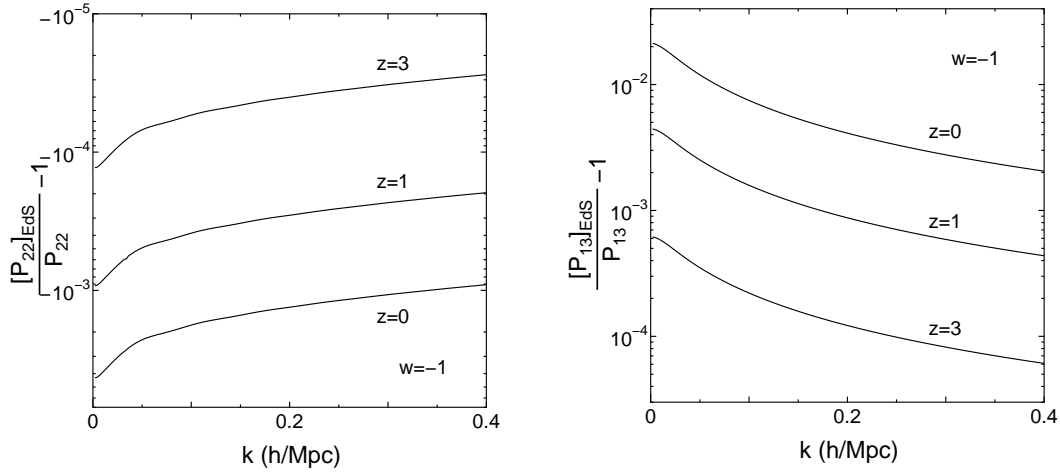


Fig. 4. Same as top panels in Fig.3, but at various redshifts of $z = 0, 1, 3$.